Challenges of Microsimulation Calibration with Traffic Waves using Aggregate Measurements

Sadman Ahmed Shanto[1,2], G. Gunter[2], D. B. Work[2], R. Ramadan[3] , B. Seibold[3]
[1]Department of Physics and Astronomy, *Texas Tech University*
[2]Institute for Software Integrated Systems, *Vanderbilt University*
[3]Department of Mathematics, *Temple University*

Abstract:

This work explores the challenges associated with calibrating parameters of microscopic models with aggregate speed data, e.g., obtained from roadside sensors. Using the Intelligent Driver Model, we explore how reliably parameters that do not influence the equilibrium flow (i.e., the Fundamental Diagram), but do control the stability of those equilibria, can be determined from aggregate speed data. Using a carefully controlled computational setup, we show that standard loss functions used for calibrating microsimulation models can perform poorly when the true parameters result in an unstable traffic state. Precisely, it is found that all of the considered loss functions frequently return different and incorrect parameter sets that minimize the expected value of the loss function. These results highlight the need for improved loss functions, or even fundamental additions to the model calibration procedure.

Intelligent Driver Model (IDM):

In order to describe the trajectories of individual vehicles, each vehicle is modeled via an ordinary differential equation that either describes the vehicle velocity (first order models), or the velocity and acceleration (second-order models). Second-order car-following models are of the form

$$\dot{v}(t) = f(\boldsymbol{\theta}, s(t), v(t), \Delta v(t)) \qquad [1]$$

The IDM is a special case of [1] and reads

$$f(\boldsymbol{\theta}, s, v, \Delta v)_{\text{IDM}} = a\left[1 - \left(\frac{v}{v_0}\right)^{\delta} - \left(\frac{s^*(v, \Delta v)}{s}\right)^2\right] \qquad [2]$$

where $s^*(v, \Delta v)$ is given by [3]

$$s^*(v, \Delta v) = s_0 + vT + \frac{\max\{0, v\Delta v\}}{2\sqrt{ab}} \qquad [3]$$

IDM and the Fundamental Diagram (FD):

Road traffic is always in a specific state that is characterized by *the flow rate*, *traffic density* and *the mean speed*. We combine all the possible homogeneous and stationary traffic states in an equilibrium function that can be described graphically by three diagrams known as the Fundamental Diagram. IDM has been shown to have robust fit when compared to measured controlled traffic data,.(Fig. 1).

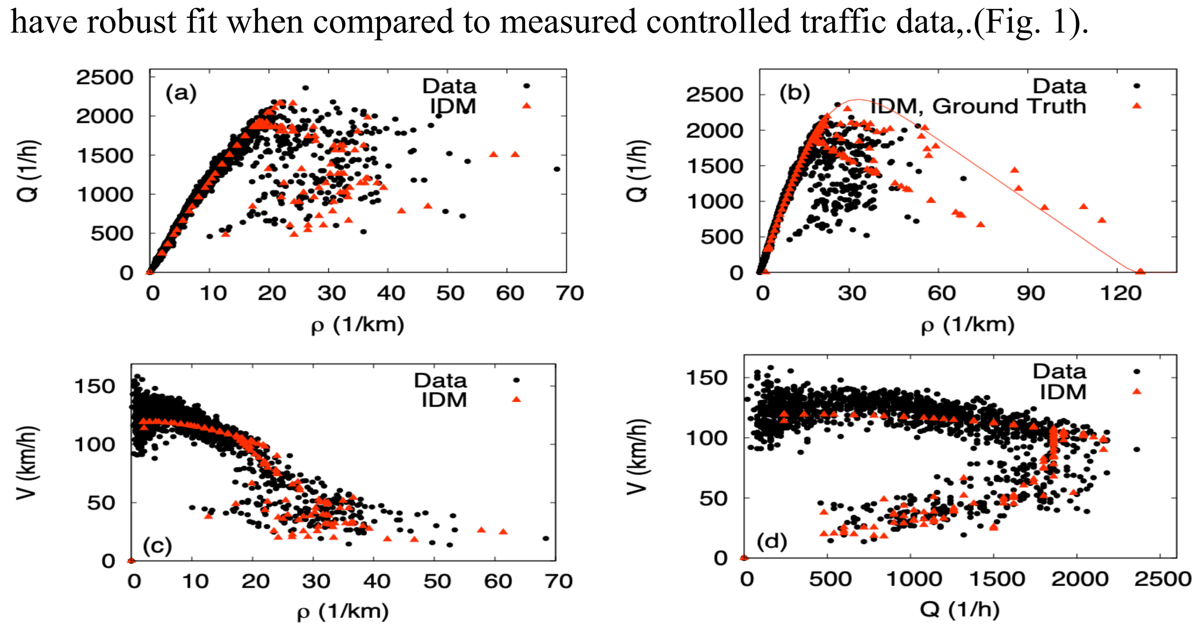

FIGURE 1: Fit of IDM on real data

We have shown that under equilibrium conditions, the factors a and b do not affect the shape of the FD. Put differently, this means finding the equilibrium spacing function $s_{eq}(v)$, that gives an equilibrium spacing value for a given speed. For $a > 0$, the equilibrium spacing function reads

$$s_{eq}(v) = \sqrt{\frac{s_0 + vT}{1 - \left(\frac{v}{v_0}\right)^{\delta}}} \qquad [4]$$

Calibration Problem and Objective Function:

Microscopic calibration commonly means that a certain model structure is postulated with a handful of free parameters that are to be fitted so that the model reproduces available measurement data suitably well. Specifically, the "best fit" parameters are determined as the solution of an optimization problem of the form:

$$\underset{\boldsymbol{\theta}}{\text{minimize}} \quad L(Y_{\text{real}}, Y_{\text{sim}}(\theta, \lambda)) \qquad [5]$$

where θ are the free decision variables to be determined, λ are (non-free) hyper-parameters that are known a-priori, Y_{real} are the measurement data Y_{sim} are the corresponding data generated by a stochastic simulated model under a given parameter choice and L is a loss function that defines a suitable distance between data and model prediction. While the data is range agnostic, in this work, however, we use macroscopic measurements (e.g., from roadside sensors such as inductive loops or radar units) as our input data. Moreover, we restrict to car-following calibration, i.e., we do not consider perimeters associated with origin destination calibration or lane changing logic.

Simulation Experiment:

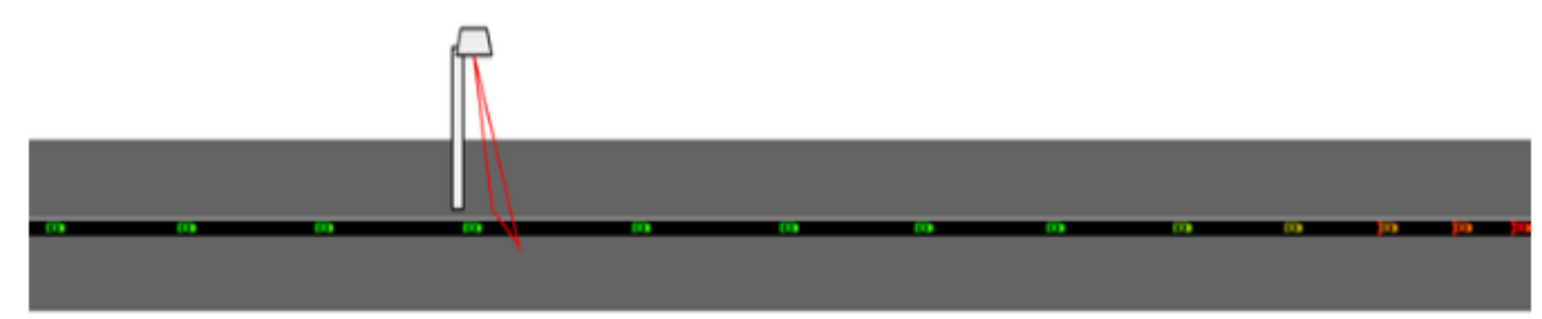

FIGURE 2 : A graphic representing the road geometry combined with a single radar sensor generating aggregate speed measurements.

IDM PARAMETERS	$v_0 = 30$; $T = 1$; $s_0 = 2$; $\delta = 4$; $\sigma = 0.1$
NETWORK GEOMETRY	Single lane road of length 2100 m with a single sensor placed at $x = 500\ m$
TRAFFIC FLOW CONDITIONS	*Free flow inflow rate = 2250 vehicles/hour*; *Congested outflow rate =1600 vehicles/hour*
SIMULATOR SETTINGS	*Simulator:* Flow; *Run time:* 1800 s; *fidelity:* 30 s; *step:* 0.4 s; *# per sim:* 50
OPTIMIZER STUDIED	Nelder-Mead (*Best*), Least Squares, SLSQP, Powell, Newton-CG, COBYLA

TABLE 0: Summary of simulation set up and settings

Methodology:

Given the simplified experimental setting described above, the resulting calibration problem stated in (1) amounts to $\boldsymbol{\theta}$ containing only a and b, which can then be compared to the true a and b used to generate the data. In order to isolate the consequences of the loss function from the consequences of the optimization solver, here we adopt a brute force parameter sweep solution approach (which is costly but it eliminates any error in the optimization procedure itself). Namely we consider solving the optimization problem on a fixed grid in the (a, b) parameter space, by varying the parameters in increments of 0.1 within ranges of [0.5, 1.3] and [1.0, 1.5] respectively (with units m/s2, for simplicity omitted here and below). As we will illustrate in the Results section, the loss function hinders the ability to correctly calibrate the model, even when solved via a brute force approach. To evaluate the loss function under a given parameter set $\boldsymbol{\theta}$, suppose a total of M simulations are conducted. Then, the effective loss function between the simulated data for this $\boldsymbol{\theta}$ and real data is given by [6] .

$$\hat{L}\,(Y_{real}, Y_{\boldsymbol{\theta}}) = \frac{1}{M}\sum_{i=1}^{M} L(Y_{real}, Y_{\boldsymbol{\theta}}^{j}) \qquad [6]$$

Loss Function Name	Abbreviation	Function Definition
Mean error	L_{ME}	$\frac{1}{N}\sum_{i=1}^{N}(Y_{sim}(i) - Y_{real}(i))$
Mean normalized error	L_{MNE}	$\frac{1}{N}\sum_{i=1}^{N}\frac{Y_{sim}(i)-Y_{real}(i)}{Y_{real}(i)}$
Root mean normalized squared error	L_{RMSNE}	$\sqrt{\frac{1}{N}\sum_{i=1}^{N}\left(\frac{Y_{sim}(i)-Y_{real}(i)}{Y_{real}(i)}\right)^2}$
Mean absolute normalized error	L_{MANE}	$\frac{1}{N}\sum_{i=1}^{N}\frac{\lvert Y_{sim}(i)-Y_{real}(i)\rvert}{Y_{real}(i)}$
Squared sum error	L_{SSE}	$\sum_{i=1}^{N}(Y_{sim}(i) - Y_{real}(i))^2$
Root mean squared error	L_{RMSE}	$\sqrt{\frac{1}{N}\sum_{i=1}^{N}(Y_{sim}(i) - Y_{real}(i))^2}$
Mean absolute error	L_{MAE}	$\frac{1}{N}\sum_{i=1}^{N}\lvert Y_{sim}(i) - Y_{real}(i)\rvert$
Thiel's inequality coefficient	L_U	$\frac{\sqrt{\frac{1}{N}\sum_{i=1}^{N}(Y_{real}(i)-Y_{sim}(i))^2}}{\sqrt{\frac{1}{N}\sum_{i=1}^{N}(Y_{real}(i))^2}+\sqrt{\frac{1}{N}\sum_{i=1}^{N}(Y_{sim}(i))^2}}$

TABLE 1 : A summary of the loss functions considered in this study.

Results and Conclusions:

1. Influence of stochastic forcing and existence of model instability

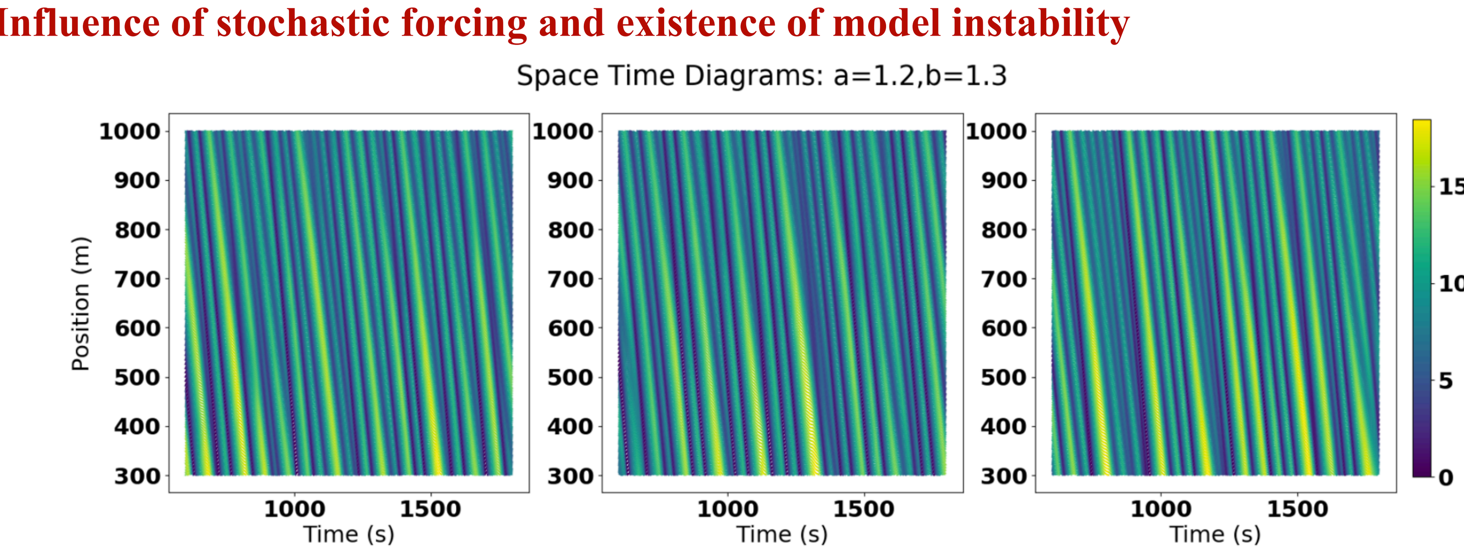

FIGURE 4: Three time space diagrams colored by speed in (m/s) produced from identical simulations except for the random seed, with $(a, b) = (1.2, 1.3)$. Waves are present and small variations occur in the phase and amplitude of the waves.

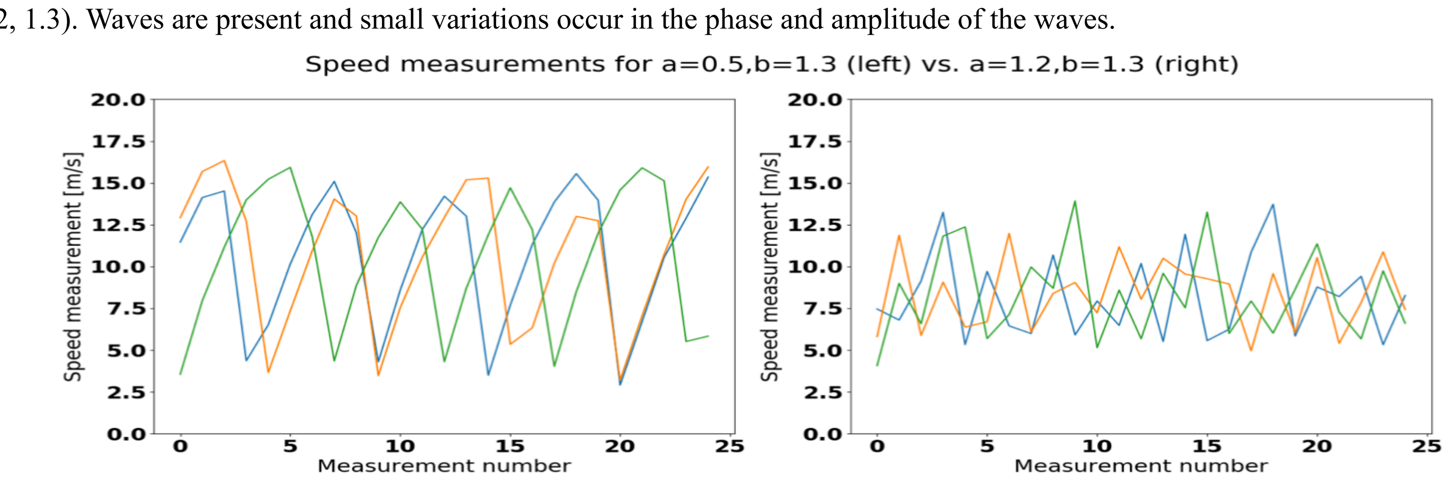

Figure 5: Illustration of the time series measurements recorded for the three simulations under $(a, b) = (0.5, 1.3)$ (left) and $(a, b) = (1.2, 1.3)$ (right).

2. RMSE loss function to recover true parameters and sensitivity to true parameters

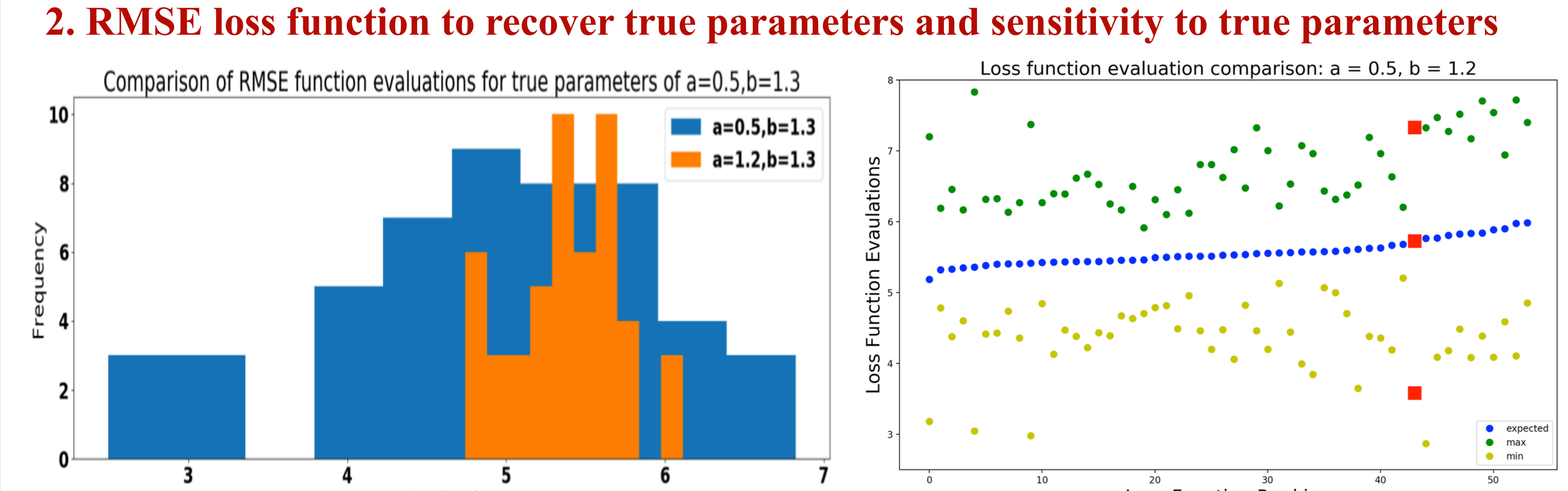

Figure 6: a) Histogram of RMSE loss function evaluations comparing a holdout $Ysim$ generated under the true parameters $(a, b) = (0.5, 1.3)$. **b)** Loss function evaluations using $LRMSE$ and a true parameter set of (a, b)=(0.5, 1.2) are shown for every parameter set, sorted by order of expected loss.

3. Performance of Various Loss Functions

Loss Function	Average % Failure	Average Divergence in a	Average Divergence in b
ME:	49.1	0.40	0.25
MNE:	49.0	0.40	0.25
RMSNE:	47.5	0.39	0.24
MANE:	47.1	0.37	0.24
SSE:	44.4	0.28	0.20
RMSE:	43.5	0.26	0.17
MAE:	42.1	0.24	0.19
U:	31.4	0.19	0.18

TABLE 2 : Reporting of three different error metrics on each candidate loss function. All loss functions are found to have similar and high degrees of error in their performance.

Acknowledgements

This material is based upon work supported by the National Science Foundation under Grant CNS-1837652, and work supported by the U.S.\Department of Energy's Office of Energy Efficiency and Renewable Energy (EERE) under the Vehicle Technologies Office award number CID DE-EE0008872. The views expressed herein do not necessarily represent the views of the U.S. Department of Energy or the United States Government.

VANDERBILT UNIVERSITY ISIS

TEXAS TECH UNIVERSITY Department *of* Physics & Astronomy